Glycative Stress Research

Online edition : ISSN 2188-3610
Print edition : ISSN 2188-3602
Received : August 3, 2023
Accepted : September 5, 2023
Published online : September 30, 2023
doi:10.24659/gsr.10.3_94

Original article

Diverse effects of single molecules of rice-derived functional lipids, glucosylceramides, ceramides, and β-sitosterol glucoside, on epidermal and lung functions

Hiroshi Shimoda [1], Shogo Takeda [1], Kenchi Miyasaka [1], Akari Yoneda [1], Yoshiaki Manse [2], Toshio Morikawa [2,3]

1) R&D, Oryza Oil & Fat Chemical Co., Ltd., Aichi, Japan
2) Pharmaceutical Research and Technology Institute, Kindai University, Osaka, Japan
3) Antiaging Center, Kindai University, Osaka, Japan

Abstract

Glucosylceramides (GlcCer), ceramides (Cer), and β-sitosterol glucoside (BSG) are produced in the refining process of rice bran oil. GlcCer are used for functional foods that claim to promote skin barrier functions and moisturization. However, the efficacies of single molecules of GlcCer, Cer, and BSG remain unclear. Therefore, we herein examined the effects of rice-derived GlcCer, Cer, and BSG on skin. The anti-inflammatory effects of BSG in a mouse pneumonia model were also investigated. Skin barrier effects were assessed based on transepidermal water loss (TEWL) in a reconstructed human epidermal keratinization model. The results obtained showed that GlcCer[d18:2(4*E*,8*Z*)] with C18 to C26 fatty acids, Cer[t18:0/24:0], and BSG decreased TEWL. The suppressive effect of GlcCer was dependent on the length of fatty acids, while Cer[t18:0/24:0] and GlcCer[d18:2(4*E*,8*Z*)/26:0] exerted similar strong effects. GlcCer[d18:2(4*E*,8*Z*)] with C18 and C20 fatty acids and Cer[t18:0/24:0] suppressed melanogenesis in B16 melanoma cells. Furthermore, BSG prolonged the survival of influenza-infected mice and increased blood O_2 saturation in lipopolysaccharide-induced pneumonia mice. In conclusion, GlcCer promoted barrier function in a fatty acid length-dependent manner and up-regulated the expression of filaggrin. Cer[t18:0/24:0] strongly promoted barrier functions by increasing the production of Cer[NS/NDS]. GlcCer[d18:2(4*E*,8*Z*)] with C18 and C20 fatty acids and Cer[t18:0/24:0] suppressed melanogenesis. These results suggest that specific GlcCer and Cer promote epidermal barrier functions and exhibit anti-melanogenic activity, leading to clinical efficacy. BSG also contributed to epidermal and lung barrier functions. Therefore, these 3 components in rice oil by-products are beneficial for skin and lung health.

***KEY WORDS*:** glucosylceramide; β-sitosterol glucoside; transepidermal water loss; melanin; pneumonia

Introduction

Glucosylceramides (GlcCer) and β-sitosterol glucoside (BSG) concomitantly exist in a wide variety of plants [1] and exert beneficial effects on health. As functional foods in Japan, GlcCer are added to processed foods to promote epidermal moisturization and barrier function [2]. A clinical study suggested the potential of rice-derived GlcCer and BSG to suppress transepidermal water loss (TEWL), which reflects skin barrier functions [3]. An increase in the epidermal production of ceramide (Cer) by GlcCer supplementation has been suggested as one of the mechanisms responsible for their promotion of barrier functions [4]. Skin Cer are sphingolipids that mainly exist in the stratum corneum (SC) and play pivotal roles in epidermal hydration and barrier functions [5] with other lipids, including cholesterol, and moisturizing proteins, such as filaggrin [6]. Among Cer, ω-hydroxy Cer, such as Cer[EOS], which has very long chain fatty acids, are essential for skin barrier functions [7]. In addition, a recent study demonstrated that Cer[NP] was more important than Cer[NS], the most abundant Cer in SC [8].

Plant-derived GlcCer consist of a sphingoid base and between C16 and C26 fatty acids depending on the plant. Besides GlcCer, Cer without a glucose in their structure,

Correspondence to: Hiroshi Shimoda
Numata 1, Kitagata-cho, Ichinomiya, Aichi 493-8001, Japan,
TEL: +81-586-86-5141 FAX: +81-586-86-6191
e-mail: kaihatsu@mri.biglobe.ne.jp
Co-aouthors; Takeda S, kaihatsu@mri.biglobe.ne.jp;
Miyasaka K, kaihatsu@mri.biglobe.ne.jp; Yoneda A, kaihatsu@mri.biglobe.ne.jp;
Manse Y, manse@phar.kindai.ac.jp; Morikawa T, morikawa@kindai.ac.jp

including Cer[t18:0/24:0] (ceramide[AP]), have been identified as minor constituents in rice [9] and several fermented foods [10]. However, limited information is currently available on the effects of single molecules of GlcCer and Cer on barrier functions. Therefore, we isolated 13 GlcCer and 6 Cer from the gummy by-products of rice bran oil and examined their effects on epidermal barrier [11] and melanogenesis [9] to elucidate structure-activity relationships. BSG is a glucoside of β-sitosterol that exerts beneficial effects on health, such as reductions in cholesterol [12] and lung protective effects against influenza infection [13]. However, few studies have investigated the biological effects of BSG even though it is present at approximately the same amount as GlcCer in rice. Therefore, we also investigated the epidermal and lung barrier functions of BSG.

Methods

Preparation of GlcCer and Cer

GlcCer and Cer (***Fig. 1***) were purified according to our previously described methods [3, 9, 11]. The crude GlcCer fraction manufactured from gummy by-products obtained during the refining process of rice bran oil was used as a starting material. The fraction (10 g) was applied to flash column chromatography (Yamazen, Osaka, Japan) equipped with a silica gel column (Universal silica gel column, 3L) and evaporative liquid scattered detector (ELSD, Yamazen). After washing the column with hexane: ethyl acetate (9 : 1 → 0 : 10) to remove less polar fractions, the mobile phase was changed to chloroform and methanol. The composition of the solvent was gradually changed from chloroform and methanol (10 : 1 → 0 : 10) to obtain a chloroform: methanol (8 : 2) fraction as the GlcCer fraction. The fraction was separated and repeatedly purified by HPLC equipped with an ODS column (Inertsil Prep. ODS φ20 × 250 mm, GL Science, Tokyo, Japan) and RI detector (Shimazdu RID-20A, Kyoto, Japan). Methanol was used as the solvent. HPLC fractions were evaporated to obtain GlcCer [d18:2(4*E*, 8*Z*)/18:0] (**1**, 23.6 mg), GlcCer[t18:1(8*Z*)/20:0] (**2**, 16 mg), GlcCer[d18:2(4*E*, 8*Z*)/20:0] (**3**, 117.6 mg), GlcCer [d18:2(4*E*, 8*E*)/20:0] (**4**, 56.5 mg), GlcCer[t18:1(8*Z*)/22:0] (**5**, 32.2 mg), GlcCer[d18:1(4*E*)/20:0] (**6**, 6.0 mg), GlcCer [d18:2(4*E*, 8*Z*)/22:0] (**7**, 29.1 mg), GlcCer[d18:2(4*E*, 8*E*)/22:0] (**8**, 4.5 mg), GlcCer[t18:1(8*Z*)/24:0] (**9**, 5.8 mg), GlcCer [d18:2(4*E*, 8*Z*)/24:0] (**10**, 28.7 mg), GlcCer[d18:2(4*E*, 8*E*)/24:0] (**11**, 8.9 mg), GlcCer[t18:1(8*Z*)/26:0] (**12**, 8.8 mg), and GlcCer[d18:2(4*E*, 8*Z*)/26:0] (**13**, 3.9 mg).

To obtain Cer, the chloroform: methanol (9 : 1) fraction of flash chromatography was purified by HPLC equipped with a same column described above and MeOH : tetrahydrofuran (9 : 1) as the mobile phase to obtain Cer[t18:0/24:0] (**14**, 9.9 mg), Cer[t18:0/22:0] (**15**, 6.2 mg), Cer[t18:0/23:0] (**16**, 7.4 mg), Cer[t18:0/25:0] (**17**, 4.6 mg), Cer[t18:1(8*Z*)/24:0] (**18**, 5.1 mg), and Cer[t18:0/26:0] (**19**, 5.5 mg). Chemical structures were identified by ^{1}H- and ^{13}C-NMR spectra with the referenced values [3, 9, 11].

Evaluation of Skin Barrier Function in Reconstructed Human Epidermal Keratinization (RHEK) Model by Measuring TEWL

According to the previously described methods [11, 14], A RHEK model (LabCyte EPI-MODEL) were cultured in a 24-well culture plate with assay medium under the cup. After incubating the plate at 37 °C under a 5% CO_2 atmosphere for a day, the RHEK model was treated with solutions of GlcCer (**1-13**), Cer (**14-19**) or BSG (final DMSO concentration: 0.1%). Culture times were selected for each experiment. The RHEK model was cultured for 7 days and then subjected to TEWL measurements, a lipid analysis, Western blotting, and microscopic observations, or for 2 days followed by real-time RT-PCR.

TEWL measurements were conducted before and 1, 3, 5, and 7 days after the treatment of samples with Tewitro TW24 (Courage+Khazaka, Cologne, Germany). The RHEK model was placed on a thermal insulation mat (HIENAI Mat; Cosmo Bio Co., Ltd., Tokyo, Japan), which maintained the entire bottom surface at 32 °C, without a lid for 5 min before measurements. TEWL was measured for 30 min while maintaining the bottom surface at 32 °C, and the mean value for the last 10 min was used in the analysis. Measurements were performed under sterile conditions.

Skin Cer Identification and Determination

According to our previously described methods [11, 14]. SC lipids from the RHEK model were extracted using a mixture of chloroform, methanol, and PBS (1 : 2 : 0.8). Dried SC lipid samples were subjected to HPTLC to measure Cer contents.

Real Time RT-PCR and Western Blotting Analysis

The mRNA expression of Cer synthesis-related enzymes in the RHEK model was measured by quantitative real time RT-PCR according to our previously described method [11, 14]. Extracted RNA from the whole RHEK model was reverse-transcribed to obtain cDNA.

The Western blot analysis described in our previous studies [11, 14] was used to assess protein expression. Proteins extracted from the RHEK model were electrophoresed on 10% SDS gels and then separated proteins were transferred to polyvinylidene difluoride membranes. After blocking with 5% skim milk, membranes were treated with a primary antibody followed by a secondary antibody. Anti-GCS (1 : 200), anti-filaggrin (1 : 200), anti-corneodesmosin (1 : 200), anti-CerS3 (1 : 1,000), anti-GCS (1 : 200), and anti-GAPDH (1 : 1,000) antibodies were used as primary antibodies. HRP-conjugated goat anti-rabbit IgG (1 : 5,000) and HRP-conjugated goat anti-mouse IgG (1 : 5,000) were used as secondary antibodies. SuperSignal™ West Pico PLUS Chemiluminescent Substrate and SuperSignal™ West Femto Maximum Sensitivity Substrate were used for detection solutions.

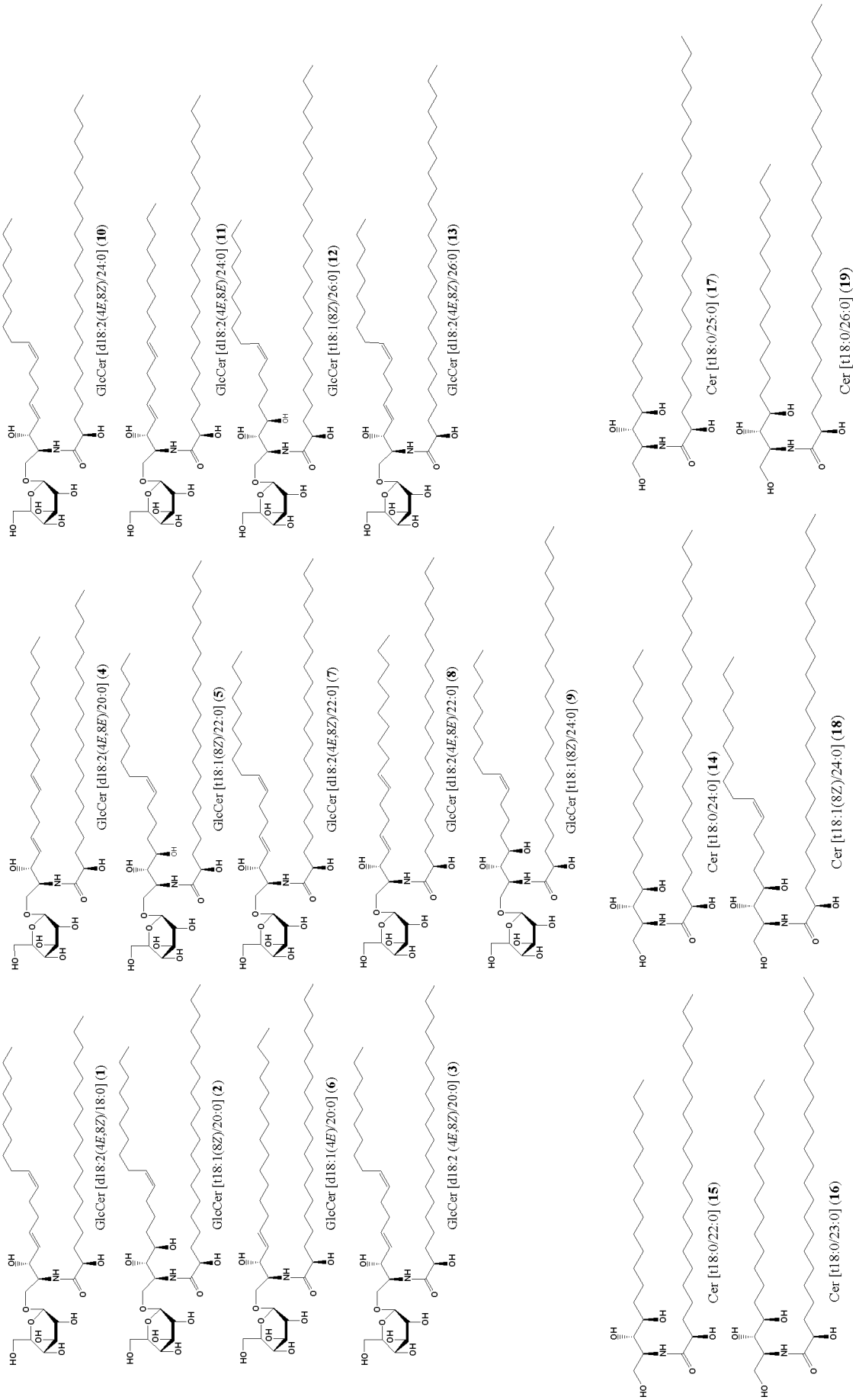

Fig. 1. **Structures of rice-derived GlcCer (1-13) and Cer (14-19).**

Cer, ceramides; GlcCer, glucosylceramides.

Electron Microscopic Analysis

Regarding electron microscopic observations of tissues, the preparation and imaging of pathological sections were consigned to Hanaichi UltraStructure Research Institute, Co., Ltd. (Aichi, Japan)[11].

Diet-induce Atopic Dermatitis Model in Mice

The experiment was performed in accordance with the Guidelines for Animal Experimentation (Japan Association for Laboratory Animal Science, 1987). Male hairless mice (Hos:HR-1) aged 6 weeks old were fed a special diet (HR-AD diet; Nosan Corp., Yokohama, Japan)[15] for 80 days. For normal group, standard CE-2 non-purified diet was used. At the same time as the feed was given, GlcCer (10 mg/kg) or BSG (10 mg/kg) suspended with 5% gum Arabic in water was orally given to mice once a day for 80 days. TEWL and epidermal moisture on dorsal area were measured by Vapometer (Keystone scientific Inc., Tokyo, Japan) and corneometer (Courage+Khazaka Electronic GmbH, Köln, Germany), respectively. For skin filaggrin determination, protein solution extracted from the skin were electrophoresed and adopted to Western blotting as described above. Anti-filaggrin (1:1,000) and anti-GAPDH (1:1,000) antibodies were used as primary antibodies.

Melanogenesis and mRNA Expression in B16 Melanoma Cells

B16 melanoma cells (5×10^4 cells/mL) were seeded on a 48-well culture plate (200 µL for melanogenesis) and a 24-well culture plate (500 µL for RT-PCR). After an incubation for 24 h, test samples and theophylline (2 mM) were added and incubated for 72 h. After a further incubation, medium was removed from the 48-well plate and distilled water (100 µL/well) was added. Cells were sonicated and 6 N NaOH (20 µL/well) was added. The absorbance of the sonicated solution was measured with a microplate reader (measurement wavelength: 405 nm, reference wavelength: 660 nm).

The mRNA expression was assessed by quantitative real-time RT-PCR. After extraction, 0.1 µg of total RNA was reverse transcribed using PrimeScript™ Reverse Transcriptase to obtain cDNA. Real-time RT-PCR was performed using TB Green® Premix Dimer Eraser™ and Thermal Cycler Dice® Real-Time System Single (TM 800, Takara Bio Inc.). The primers were listed in the reference[9].

Tyrosinase Inhibitory Activity and Luciferase Based ATP Assay

Crude tyrosinase solution[9] (50 µL/well, 420 µg protein/mL), a 2 mM L-DOPA (levodopa) solution (40 µL/well), and a test sample (10 µL/well) were placed onto a 96-well plate. The enzyme reaction was performed at 37 °C for 90 min. After the enzyme reaction, absorbance was measured with a microplate reader (Measurement wavelength: 475 nm, reference wavelength: 660 nm).

For luciferase assay, B16 melanoma cells (1.0×10^5 cells/mL) were seeded on a 96-well plate (100 µL/well) and incubated for 24 h. Medium was then replaced with that containing theophylline (2 mM) and the test sample. After an incubation for 24 h, medium was removed and cells were gently washed with PBS (–). ATP was determined by Glo Lysis Buffer (Promega, Madison, WI, USA) and ATP assay reagent.

Clinical Examination of UV-induced Inflammation and Pigmentation

This randomized, placebo-controlled, double-blind, parallel-group study was performed according to the Declaration of Helsinki (2013 revision) and was registered in the University Hospital Medical Information Network Clinical Trials Registry (UMIN000042696). Inclusion criteria were Japanese male and female adults (20 years or older and 59 years or younger) with a normal skin color or fair skin who expressed concerns about dry skin. First selection criteria were individuals with confirmed minimum erythema dose 1 (MED) among 6 UV irradiated areas. Forty-eight subjects were selected for the present study. Subject allocation was performed in a manner to prevent significant differences in the means of 1 MED and forearm TEWL between groups.

Subjects took one appropriate capsule (Oryza Ceramide® or placebo) daily after breakfast for 8 weeks. Active capsules contained 40 mg of Oryza Ceramide®-PCD (comprising 1.2 mg of GlcCer and 0.06 mg of Cer[t18:0/24:0]) and 160 mg of γ-cyclodextrin. Placebo capsules contained 200 mg of γ-cyclodextrin. MED and the minimal tanning dose (MTD) were examined at baseline and after 4 and 8 weeks of the intervention as the primary outcome. UV irradiation was performed on the screening day, baseline day, after 4 weeks, and after 8 weeks. According to references, 6 areas (areas A to F) were irradiated by UV rays using a UV solar simulator (WBS-10C×6F-5UV, Ushio Inc., Tokyo, Japan) from 1074 to 2672.4 mJ/cm^2·s at intervals of 1.2 times. The content of melanin and skin redness were measured using a mexameter (MX18, Courage+Khazaka Electronic GmbH, Köln, Germany).

Survival Rate of Influenza-infected Mice

The study was performed at Hamri Co. Ltd. (Ibaraki, Japan). Test samples were orally administered to female BALB/c mice for 7 days and the virus (mutated A/PR/8/34, 7.9×10^6 $TCID_{50}$) was then intranasally inoculated. Test samples were continuously administered once a day and the survival rate was monitored.

Lipopolysaccharide (LPS)-induced Lung Neutrophil Accumulation and Pneumonia

According to the method of Rojas *et al.*[16], BSG was orally administered to male C57BL/6 mice and LPS (1 mg/kg) was intraperitoneally injected. The lungs were removed 24 h later and specimens were fixed in 4% paraformaldehyde. The specimen for microscopic analysis was stained by H.E. For peneumonia model[17], BSG or dexamethasone was orally administered to male ICR mice from the day or the day after the intratracheal administration of LPS (75 µg). Test samples were administered once a day and oxygen saturation was measured by pulse oximeter (MouseOx, Harvard Apparatus, Hollison, MA, USA) for 3 min under anesthesia.

Results & Discussion

Effects of Rice-derived GlcCer, Cer, and BSG on Epidermal Barrier Functions

1) Skin Barrier Abilities of GlcCer and Cer

The RHEK model was treated with a sample for 7 days and TEWL was measured every 2 days. The results obtained showed that 10 μM of GlcCer with 4*E*,8*Z* sphingadienine, such as GlcCer[d18:2(4*E*,8*Z*)/18:0] (**1**), GlcCer[d18:2(4*E*/8*Z*)/20:0] (**3**), GlcCer[d18:2(4*E*/8*Z*)/22:0] (**7**), GlcCer[d18:2 (4*E*/8*Z*)/24:0] (**10**), and GlcCer[d18:2(4*E*/8*Z*)/26:0] (**13**), decreased TEWL after 7 days (***Fig. 2***, upper). Structure-activity relationships were clearly demonstrated for GlcCer [d18:2(4*E*,8*Z*)] (**1, 3, 7, 10, 13**), but not GlcCer[t18:1(8*Z*)] (**2**, **5**, **9**, **12**), GlcCer[d18:2(4*E*,8*E*)] (**4**, **8**, **11**), or GlcCer[t18:1(4*E*)] (**6**). The effects of active GlcCer (**1**, **3**, **7**, **10**, **13**) on epidermal barrier functions were dependent on fatty acid lengths, with longer carbon chains of fatty acids in GlcCer[d18:2(4*E*,8*Z*)] more strongly promoting barrier functions. The effects of **10** and **13** with more than C24 fatty acids on barrier functions were observed in the earlier stages of the culture (Days 1 and 3) and were strong.

Regarding Cer, 10 μg/mL of Cer[t18:0/24:0] (**14**), Cer [t18:0/23:0] (**16**), and Cer[t18:1(8*Z*)/24:0] (**18**) significantly reduced TEWL (***Fig. 2***, lower). However, a clear structure-activity relationship was not confirmed, such as relationships between activity and fatty acid lengths or the types of sphingoid bases. Among Cer, Cer (**14**) at 1, 3, and 10 μg/mL exerted concentration-dependent effects on barrier functions. These effects were as strong as those of GlcCer (**13**) in the later culture stage (Days 5 and 7), but did not decrease TEWL in the early culture stage. Therefore, the mechanisms underlying the effects of **13** and **14** appeared to differ.

2) Different Mechanisms for Effects of Cer (14) and GlcCer (13) on Skin Barrier Functions

We examined Cer contents in the RHEK model treated with Cer (**14**) to elucidate the mechanisms responsible for enhancements in barrier functions. Cer (**14**) increased Cer contents (***Fig. 3-a***) in the RHEK model, specifically Cer [NS/NDS][11]. Since Cer[NS/NDS] is a major Cer in SC, we examined the mRNA (***Fig. 3-b***) and protein (***Fig. 3-c***) expression of enzymes involved in the *de novo* Cer-synthesizing pathway. The results obtained showed that **14** up-regulated the expression of GlcCer synthase (GCS), which has been shown to facilitate changes from Cer to GlcCer in the stratum granulosum (SG). Therefore, **14** exerted its effects on barrier functions through Cer production based on the expression of GCS.

In contrast, since GlcCer (**13**) which suppressed TEWL (***Fig. 4-a***) did not affect Cer contents (***Fig. 4-b***), we performed an electron microscopic analysis to elucidate the underlying mechanism. The results obtained showed a denser SC image of the RHEK model treated with **13** (***Fig. 4-c***, left), suggesting stronger barrier functions than in the control RHEK model. Moreover, increases in corneodesmosomes (***Fig. 4-c***, middle) and the number and area of keratohyalin granules (***Fig. 4-c***, right) were observed in the RHEK model treated with **13**. Keratohyalin granules primary exist in SG and contribute to the cross-linking of keratin filaments, which creates a tight barrier in the epidermis[18]. These granules also produce filaggrin, a precursor of natural moisturizing factor (NMF)[19]. The Western blot analysis showed an increase in the expression of filaggrin. Therefore, **13** appeared to exert moisturizing effects by up-regulating the expression of filaggrin (***Fig.4-d***, left), thereby providing NMF to SC. In addition, the Western blot analysis revealed the up-regulated expression of corneodesmosin (***Fig. 4-d***, right). Corneodesmosin, a cell adhesion molecule, exists in corneodesmosome cores and contributes to a tight SC structure[20]. The mechanism by which **13** exerted moisturizing effects may involve corneodesmosin.

Regarding the mechanisms by which rice-derived Cer and GlcCer promote barrier functions (***Fig. 5***), the main mechanism of Cer[t18:0/24:0] (**14**) involved the SC production of Cer[NS/NDS] through the expression of GCS. In contrast, GlcCer with the 4*E*,8*Z* structure exhibited barrier functions, and longer fatty acids enhanced this effect. The mechanism of GlcCer (**13**) involved enhancing the tight structure of SC and increasing NMF production without affecting Cer contents in SC.

3) Enhanced Epidermal Barrier Functions by BSG through the Production of Cer and Filaggrin

BSG (***Fig. 6-a***) residing with GlcCer in plant resources is a sterol glucoside and the biological activities despite of which have not been examined as extensively as β-sitosterol. Therefore, we investigated the effects of BSG on epidermal barrier functions[14]. BSG suppressed TEWL in the cultured RHEK model at a later stage (Day 7) (***Fig.6-b***). The underlying mechanism involved an increase in the production of Cer [EOS] through ceramide synthase (CerS)-3 and the up-regulated expression of GCS (***Fig. 6-c, d***). Since Cer[EOS] is an acylated Cer with potent barrier function[21], strong epidermal protective effects are expected. In an *in vivo* evaluation of the effects of BSG on barrier functions using a diet-induced atopic dermatitis mouse model[22], the consecutive (80 days) oral administration of BSG (10 mg/kg) significantly increased epidermal moisture and slightly suppressed TEWL (***Fig. 6-e***), whereas GlcCer did not improve these parameters in this model. The underlying mechanism involved the up-regulated expression of filaggrin (***Fig. 6-f***). Therefore, BSG strongly enhanced barrier functions in skin.

Anti-melanogenic Effects of GlcCer and Cer

Regarding the other biological activities of GlcCer and Cer in skin, we investigated their anti-melanogenic effects on theophylline-induced melanogenesis in B16 melanoma cells[9]. ***Table 1*** shows the results obtained for GlcCer (**1-13**) and Cer (**14-19**). Regarding GlcCer, GlcCer[d18:2(4*E*,8*Z*)/18:0] (**1**) and GlcCer[d18:2(4*E*,8*Z*)/20:0] (**3**) suppressed melanogenesis with IC_{50} values less than 10 μg/mL. GlcCer[d18:2(4*E*,8*E*)/20:0] (**4**) and GlcCer[d18:1(4*E*)/20:0] (**6**) slightly suppressed melanogenesis at 10 μg/mL. However, GlcCer (**9-13**) with very long chain fatty acids did not suppress melanogenesis. Based on these results, the structure-activity relationship for the suppression of melanin synthesis markedly differed from that for skin barrier functions. The structure-activity relationship for anti-melanogenic activity currently remains unclear; however, the major GlcCer (**3**) exhibited the strongest anti-melanogenic activity among rice GlcCer (**1-13**).

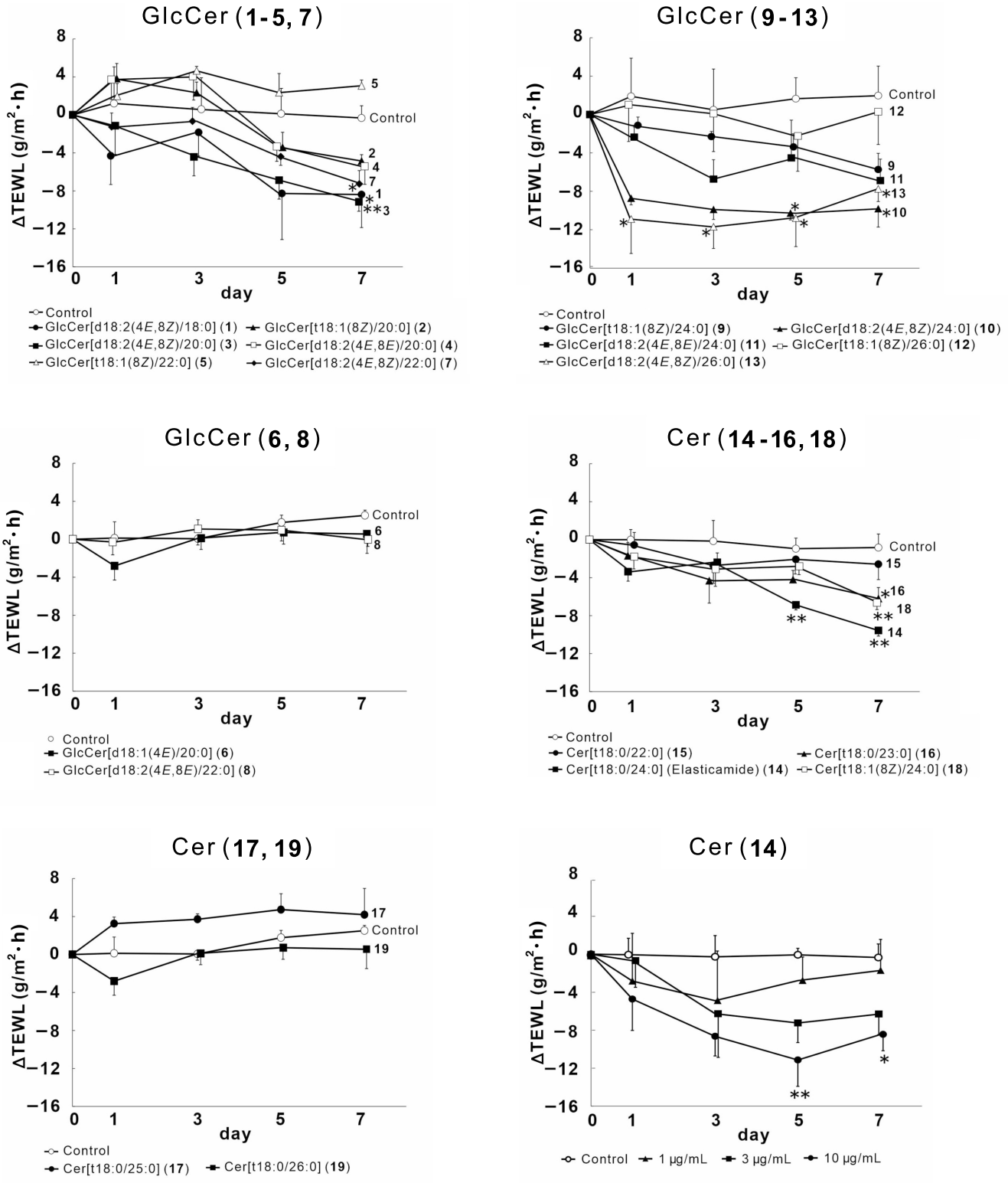

Fig. 2. **Effects of GlcCer (1-13) and Cer (14-19) on TEWL in the RHEK model.**

The RHEK model was treated with each sample (**1-13**: 10 μM, **14-19**: 10 μg/mL) for 7 days. Data are expressed as means ± SE (n = 3-4). Asterisks denote a significant difference from the control group, *p < 0.05, **p < 0.01. Figure is quoted from Ref 11. Cer, ceramides; GlcCer, glucosylceramides; TEWL, transepidermal water loss; RHEK, reconstructed human epidermal keratinization; SE, standard error.

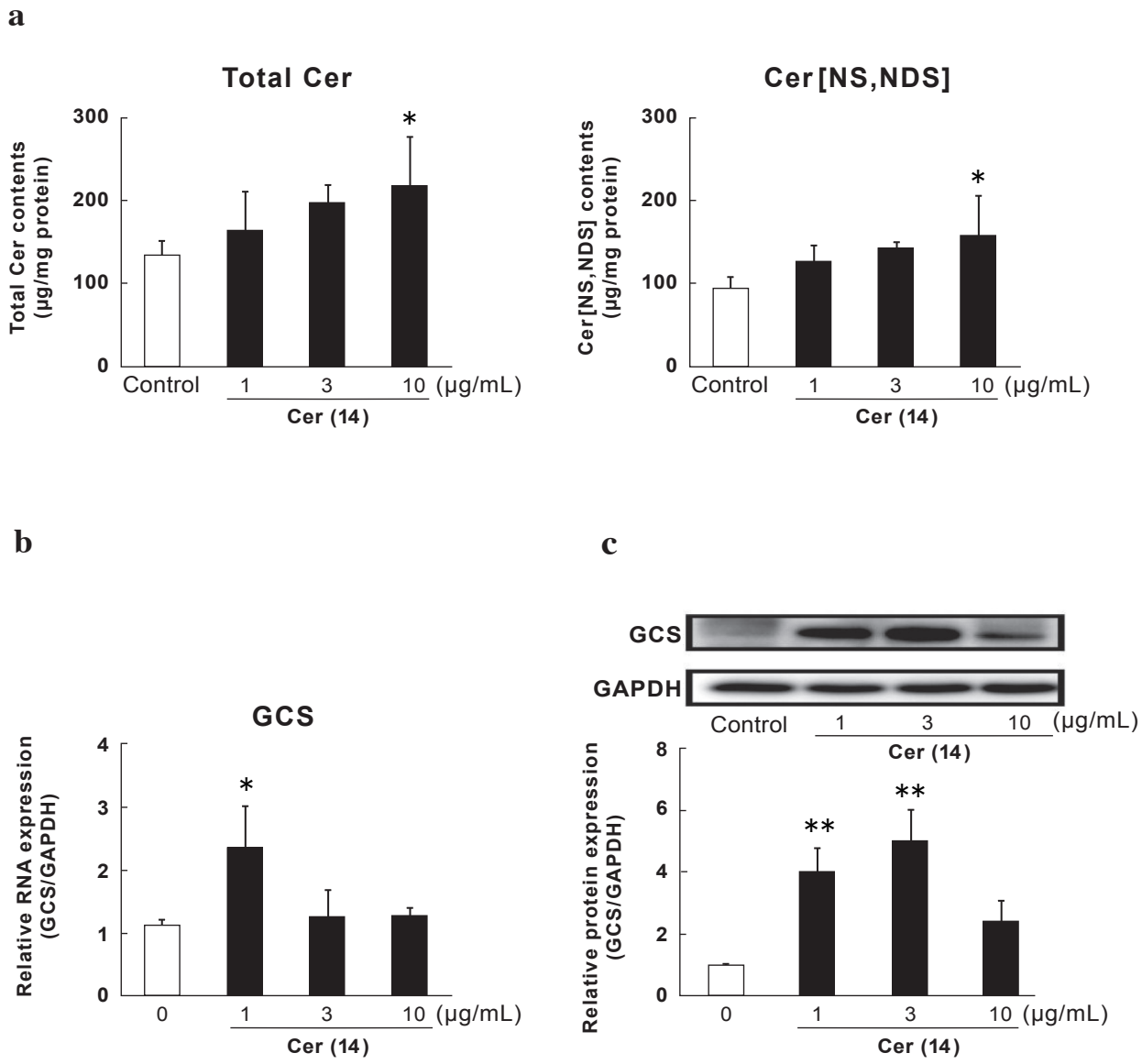

Fig. 3. **Effects of Cer (14) on ceramide contents (a) and mRNA (b) and protein (c) expression of GCS in the RHEK model.**

The RHEK model was treated for 2 days (for real-time RT-PCR) or 7 days (for ceramide contents and Western blotting) with **14** (1–10 μg/mL). Data are expressed as means ± SE (n = 4). Asterisks denote a significant difference from the control group, *p < 0.05, **p < 0.01. Figure is quoted from Ref 11. Cer, ceramides; GlcCer, glucosylceramides; GCS, GlcCer synthase; GAPDH, glyceraldehyde-3-phosphate dehydrogenase; RHEK, reconstructed human epidermal keratinization; SE, standard error.

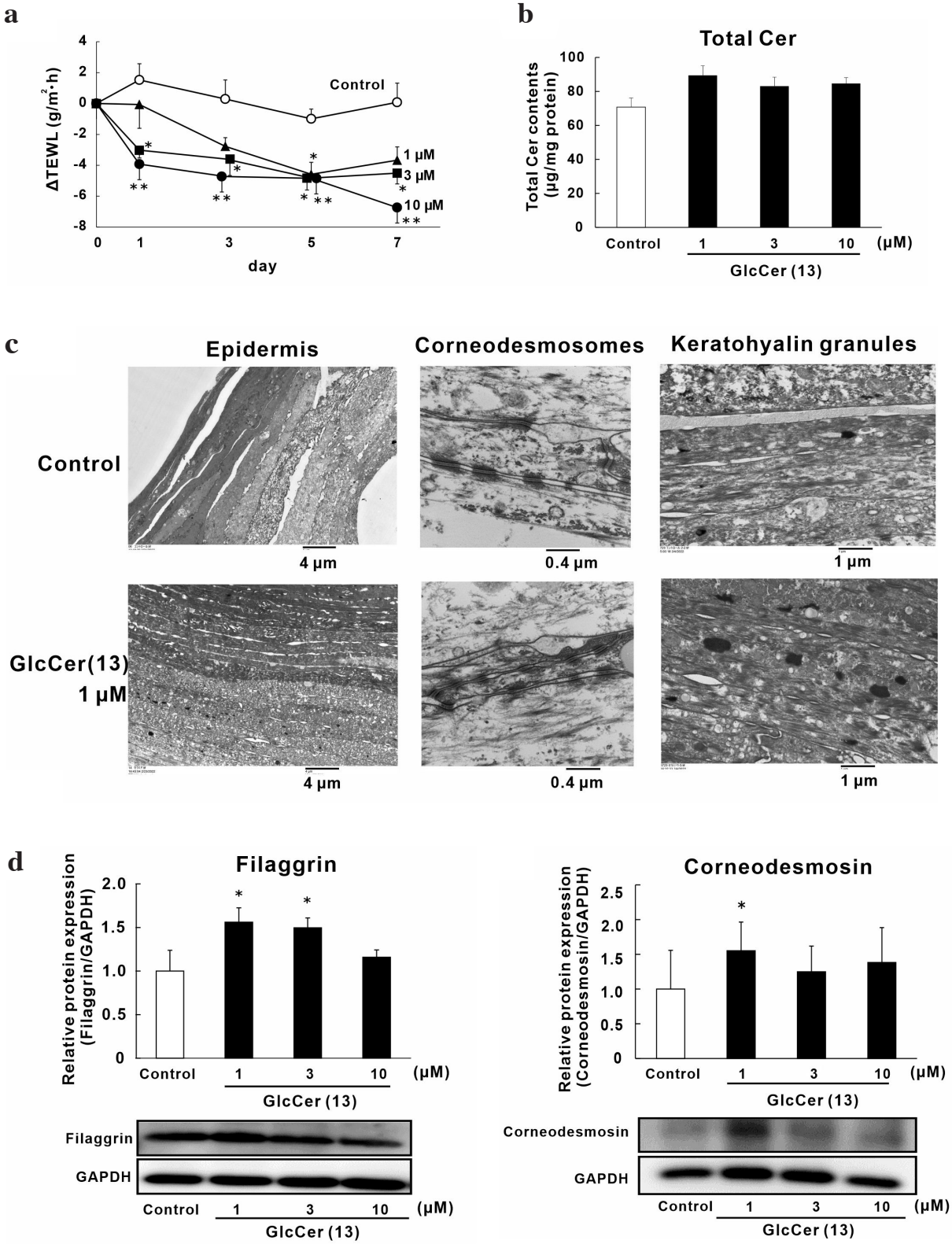

Fig.4. **Effects of GlcCer[d18:2(4*E*,8*Z*)/26:0)](13) on epidermal hydration parameters and factors in the RHEK model.**

a) Changes in TEWL, **b)** SC Cer contents after a treatment with **13** for 7 days (n = 4), **c)** electron microscopic images of cross-sections of the RHEK model, and **d)** Protein expression of filaggrin and corneodesmosin (n = 4-5). All data are expressed as means ± SE. Asterisks denote a significant difference from the control group, *p < 0.05, **p < 0.01. Figure is quoted from Ref 11. TEWL, transepidermal water loss; SC, stratum corneum; Cer, ceramides; GlcCer, glucosylceramides; GAPDH, glyceraldehyde-3-phosphate dehydrogenase; RHEK, reconstructed human epidermal keratinization; SE, standard error.

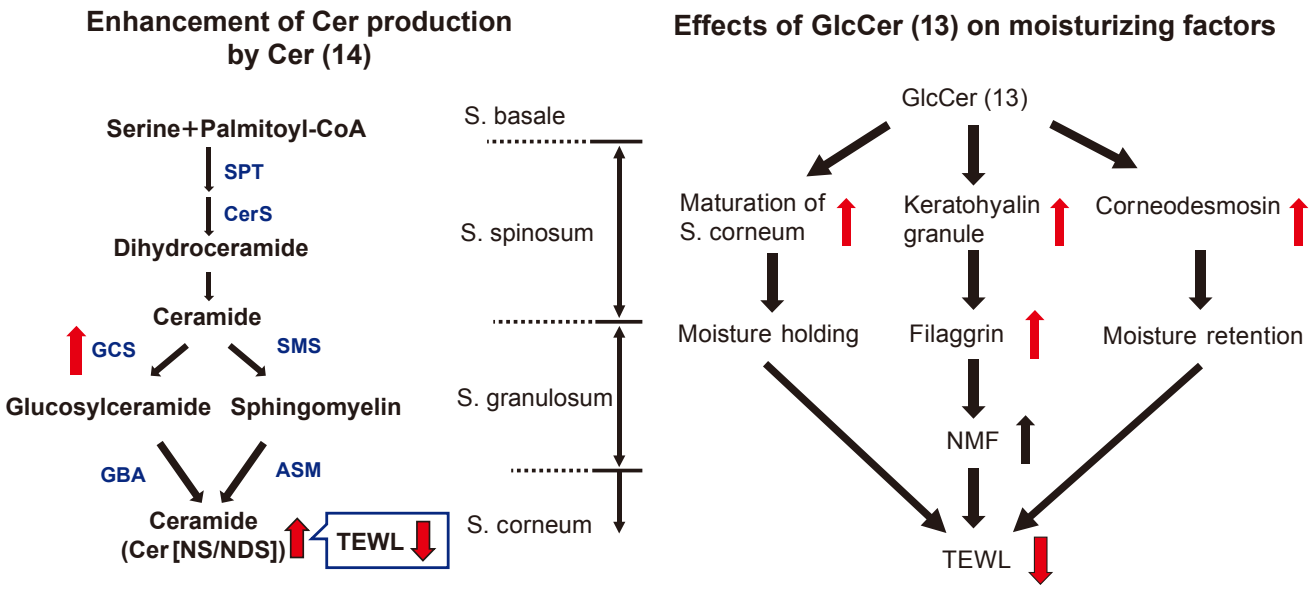

Fig. 5. **Potential mechanisms by which Cer[t18:0/24:0] (14) and GlcCer (13) promote barrier functions.**

Figure is quoted from Ref 11. Cer, ceramides; GlcCer, glucosylceramides; GCS, GlcCer synthase; SPT, serine palmitoyl-trnsferase; CerS, ceramide synthase: SMS, sphingomyelin synthase; GBA, β-glucocerebrosidase; ASM, acid sphingomyelinase; TEWL, transepidermal water loss; NMF, natural moisturizing factor.

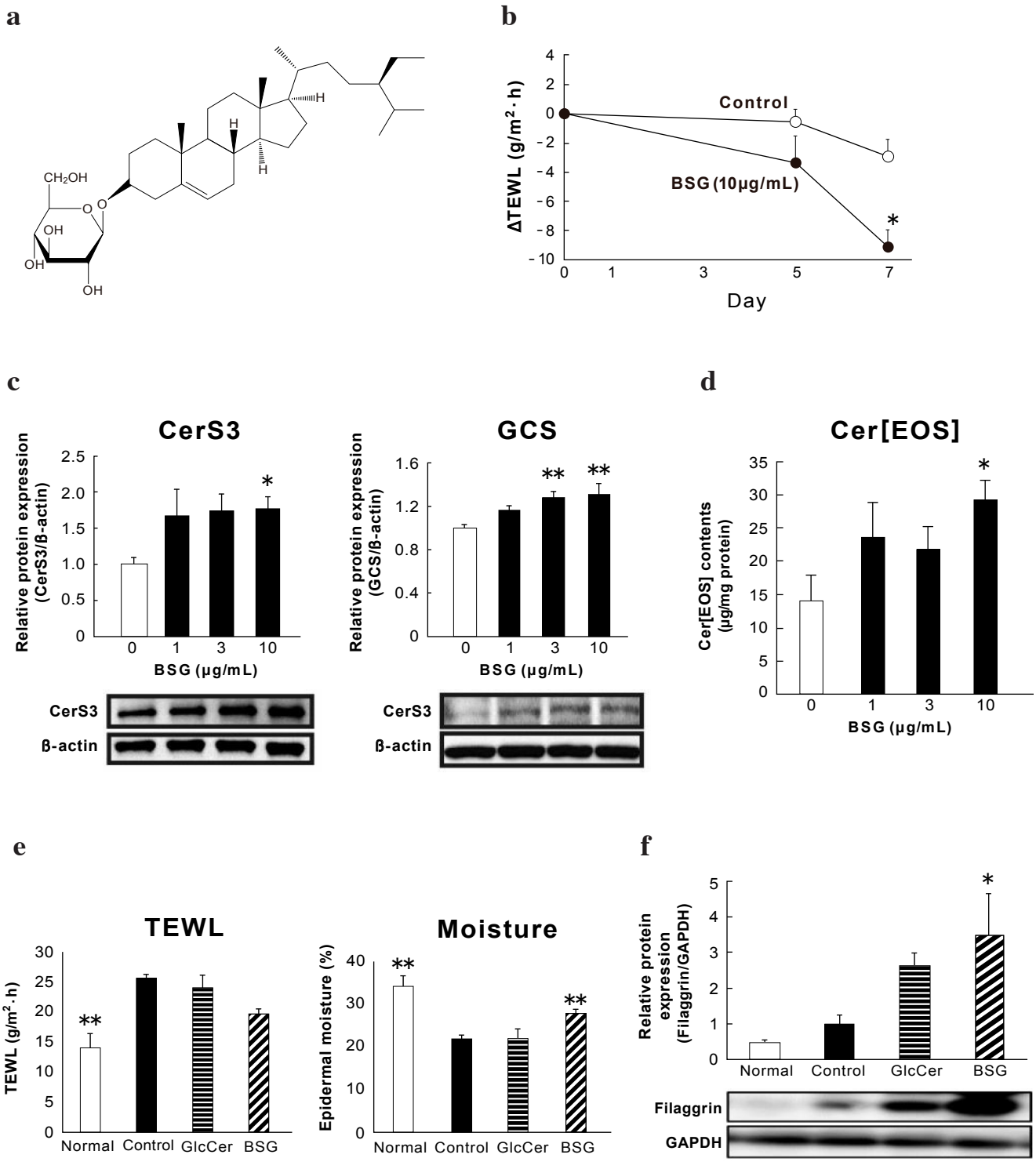

Fig. 6. **Effects of BSG on epidermal moisture and the underlying mechanism.**

a) Chemical structure of BSG. **b)** Effects of BSG on TEWL in the RHEK model (n = 4). The RHEK model was treated for 7 days with BSG (10 μg/mL). **c, d)** Effects on the protein expression of CerS3 and GCS (n = 5) and SC Cer[EOS] contents (n = 6) in the RHEK model. SC Cer[EOS] was quantified by HPTLC. **e, f)** Effects on TEWL, epidermal moisture, and filaggrin expression in diet-induced atopic disease mice (n = 3-5). BSG (10 mg/kg) or GlcCer (10 mg/kg) was orally administered to mice for 80 days and TEWL and epidermal moisture were measured. Asterisks denote a significant difference from the control group, *$p < 0.05$, **: $p < 0.01$. Figures **a**~**d** quoted from Ref. 14; **e** and **f** are unpublished original data. BSG, β-sitosterol glucoside; CerS, ceramide synthase; SC, stratum corneum; Cer, ceramides; GlcCer, glucosylceramides; GSC, GlcCer synthase; TEWL, transepidermal water loss; RHEK, reconstructed human epidermal keratinization; SE, standard error (error bar).

Table 1. Inhibitory activities of GlcCer (1-13) and Cer (14-19) on theophylline-stimulated melanogenesis of B16 melanoma cells.

	IC_{50} (μM)
GlcCer[d18:2(4*E*,8*Z*)/16:0]	NE
GlcCer[d18:2(4*E*,8*E*)/16:0]	NE
GlcCer[d18:2(4*E*,8*Z*)/18:0] (**1**)	6.6 (69.8%)
GlcCer[t18:1(8*Z*)/20:0] (**2**)	NE
GlcCer[d18:2(4*E*,8*Z*)/20:0] (**3**)	5.2 (63.4%)
GlcCer[d18:2(4*E*,8*E*)/20:0] (**4**)	>10 (45.6%)
GlcCer[t18:1(8*Z*)/22:0] (**5**)	NE
GlcCer[d18:1(4*E*)/20:0] (**6**)	>10 (32.7%)
GlcCer[d18:2(4*E*,8*Z*)/22:0] (**7**)	NE
GlcCer[d18:2(4*E*,8*E*)/22:0] (**8**)	NE
GlcCer[t18:1(8*Z*)/24:0] (**9**)	>10 (21.0%)
GlcCer[d18:2(4*E*,8*Z*)/24:0] (**10**)	NE
GlcCer[d18:2(4*E*,8*E*)/24:0] (**11**)	NE
GlcCer[t18:1(8*Z*)/26:0] (**12**)	>10 (17.8%)
GlcCer[d18:2(4*E*,8*Z*)/26:0] (**13**)	>10 (22.7%)
Cer[t18:0/24:0] (**14**)	3.9 (63.4%)
Cer[t18:0/22:0] (**15**)	NE
Cer[t18:0/23:0] (**16**)	>10 (11.7%)
Cer[t18:1(8*Z*)/24:0] (**18**)	NE
Cer[t18:0/25:0] (**17**)	NE
Cer[t18:0/26:0] (**19**)	NE

Each value represents the mean ± SE (n = 4). Values in parentheses are % inhibition of melanogenesis at 10 μg/mL. Data are quoted from Ref 9. Cer, ceramides; GlcCer, glucosylceramides; IC_{50}, half maximal inhibitory concentration; NE, not effective; SE, standard error.

Among Cer, only Cer[t18:0/24:0] (**14**) strongly suppressed melanogenesis with an IC_{50} value of 3.9 μM. The structure of **14** is the same as ceramide [AP], which is present in skin SC. Therefore, Cer[t18:0/24:0] was suggested to exert strong inhibitory effects on innate melanin production in skin.

To elucidate their mechanisms of action, we investigated whether **3** and **14** down-regulated the mRNA expression of melanogenic molecules. As shown in ***Fig. 7-a***, **14** significantly down-regulated the mRNA expression of TYRP1, whereas **3** did not. Therefore, the suppression of TYRP1 is a key anti-melanogenic mechanism of **14**. ***Fig. 7-b*** shows the effects of **3** and **14** on tyrosinase activity derived from B16 melanoma cells. Kojic acid dose-dependently inhibited tyrosinase activity (IC_{50}: 3.6 μM), whereas **3** and **14** did not. Moreover, **14** and emodin suppressed ATP levels, whereas **3** did not (***Fig. 7-c***). Therefore, the anti-melanogenic effects of **14** were attributed to reductions in TYRP1 expression and ATP levels, and not to the inhibition of tyrosinase activity. ATP is needed for the proliferation of B16 melanoma cells through P2X7 receptors [23] and melanogenesis [24]. However, the inhibitory mechanism of **3** has not yet been elucidated.

We evaluated the clinical anti-melanogenic effects of Oryza ceramide® (OC) standardized with rice lipids in a placebo-controlled double-blind study on Japanese subjects [9]. The results obtained showed that OC suppressed UV-induced skin tanning (melanin pigmentation), but not erythema. Therefore, orally administered rice GlcCer and Cer inhibited UV-induced melanogenesis (***Fig. 8***).

Effects of BSG on Influenza Virus- and LPS-induced Pneumonia in Mice

In addition to the effects of rice lipids on skin barrier functions, we examined their effects on lung protective and barrier functions in order to detect other biological activities of GlcCer and BSG. The effects of GlcCer, BSG, or a crude mixture of GlcCer and BSG were examined in mice infected with influenza virus guided by mortality. The results obtained showed that the crude mixture of GlcCer and BSG and purified BSG induced a right shift in the survival curve of mice and the average number of survival days of the mice in these groups was significantly higher (***Fig. 9-a***, left). In an additional experiment, BSG treatments induced a right shift in the survival curve (***Fig. 9-a***, right) and significantly increased the average number of survival days at 30 and 100 mg/kg. Therefore, BSG was effective against fetal pneumonia in mice induced by influenza infection.

We also investigated the potential of BSG against bactericidal pneumonia in LPS-induced mice. We intraperitoneally injected LPS and then orally administered

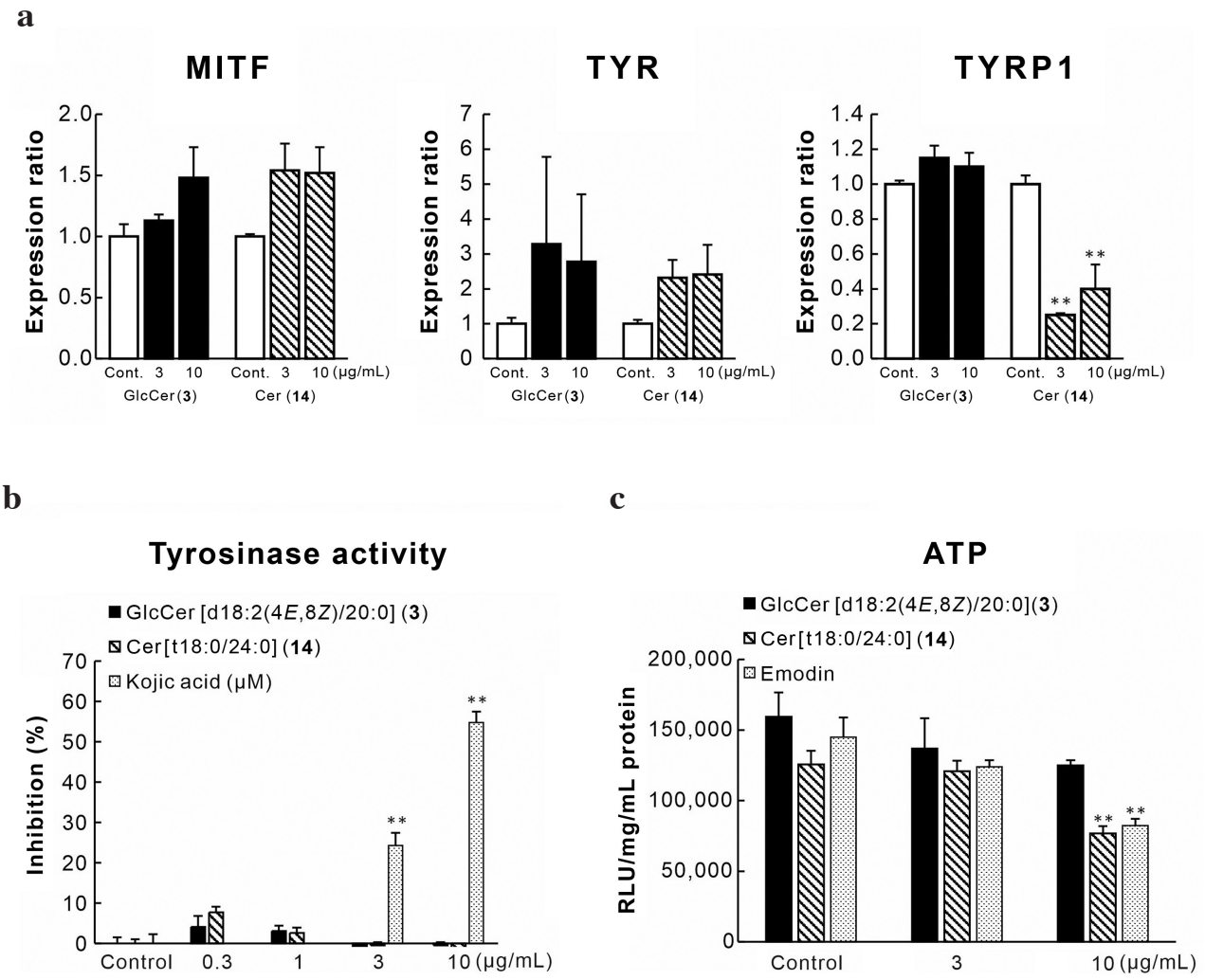

Fig. 7. **Effects of GlcCer [d18:2(4*E*,8*Z*)/20:0] (3) and Cer [t18:0/24:0] (14) on the mRNA expression of melanogenic factors (a), tyrosinase activity (b), and ATP levels in B16 melanoma cells (c).**

a) B16 melanoma cells were treated with **3** or **14** for 72 hr. Each value was corrected by the mRNA expression level of β-actin and shown as a relative value to the control. **b)** Crude tyrosinase was extracted from B16 melanoma cells treated with theophylline for 72 h. Enzyme solutions were incubated with L-DOPA and test samples for 90 min. **c)** Cells were treated with **3** or **14** for 24 h. Data are expressed as the mean ± SE (n = 4). Asterisks denote significant differences from the control at **p < 0.01. Figures are quoted from Ref 9. Cer, ceramides; GlcCer, glucosylceramides; ATP, adenosine triphosphate; L-DOPA, levodopa; MITF, melanocyte inducing transcription factor; TYR, tyrosinase; TYRP1, tyrosinase-related protein 1; SE standard error.

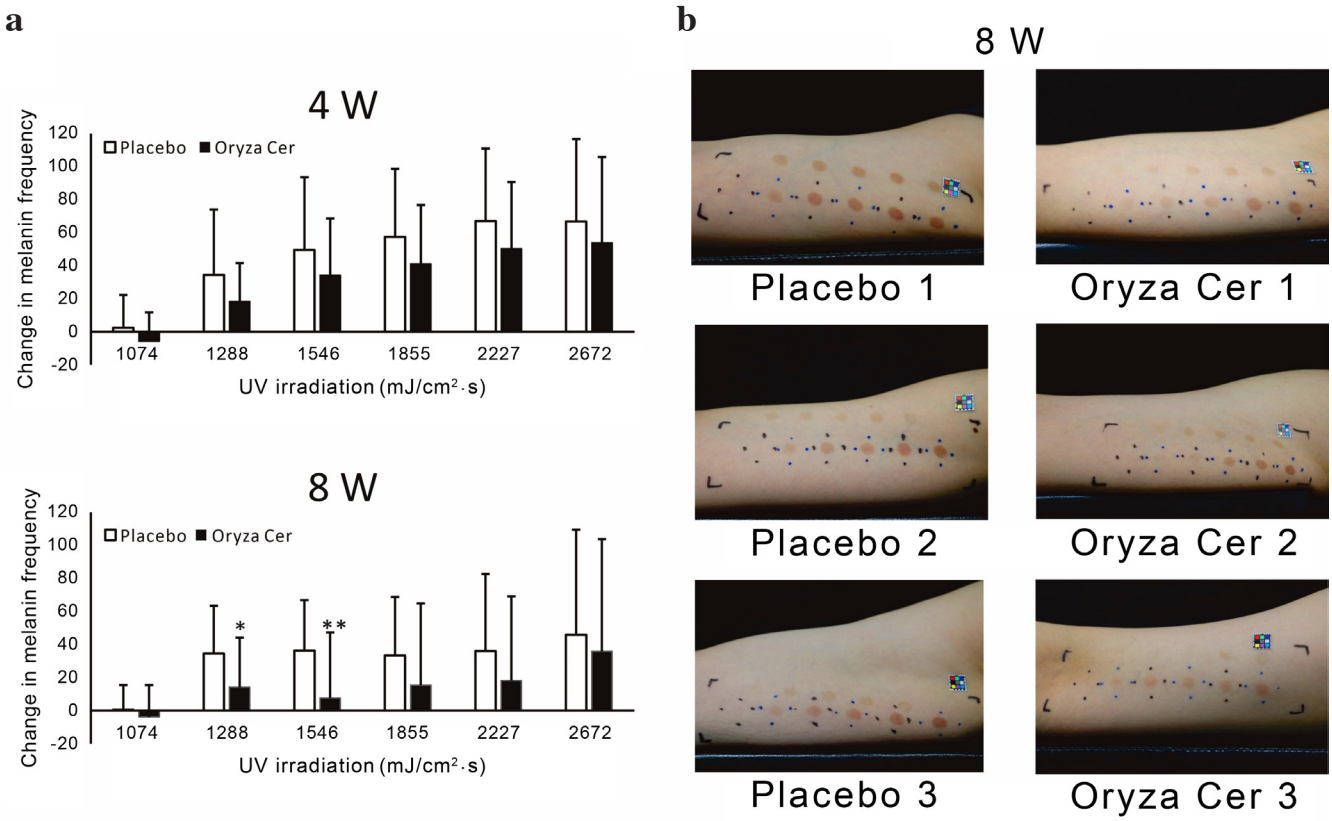

Fig. 8. **Effects of Oryza ceramide® on skin pigmentation induced by UV irradiation.**

a) Changes in melanin frequency in UV-irradiated skin. Each value represents the mean and SD (n = 24). Asterisks denote significant differences from the control at *$p < 0.05$ and **$p < 0.01$. **b)** The arm skin of 3 typical subjects in each group exposed to UV irradiation after 8 weeks. Figures are quoted from Ref 9. Cer, ceramide; UV, ultraviolet; SD, standard deviation.

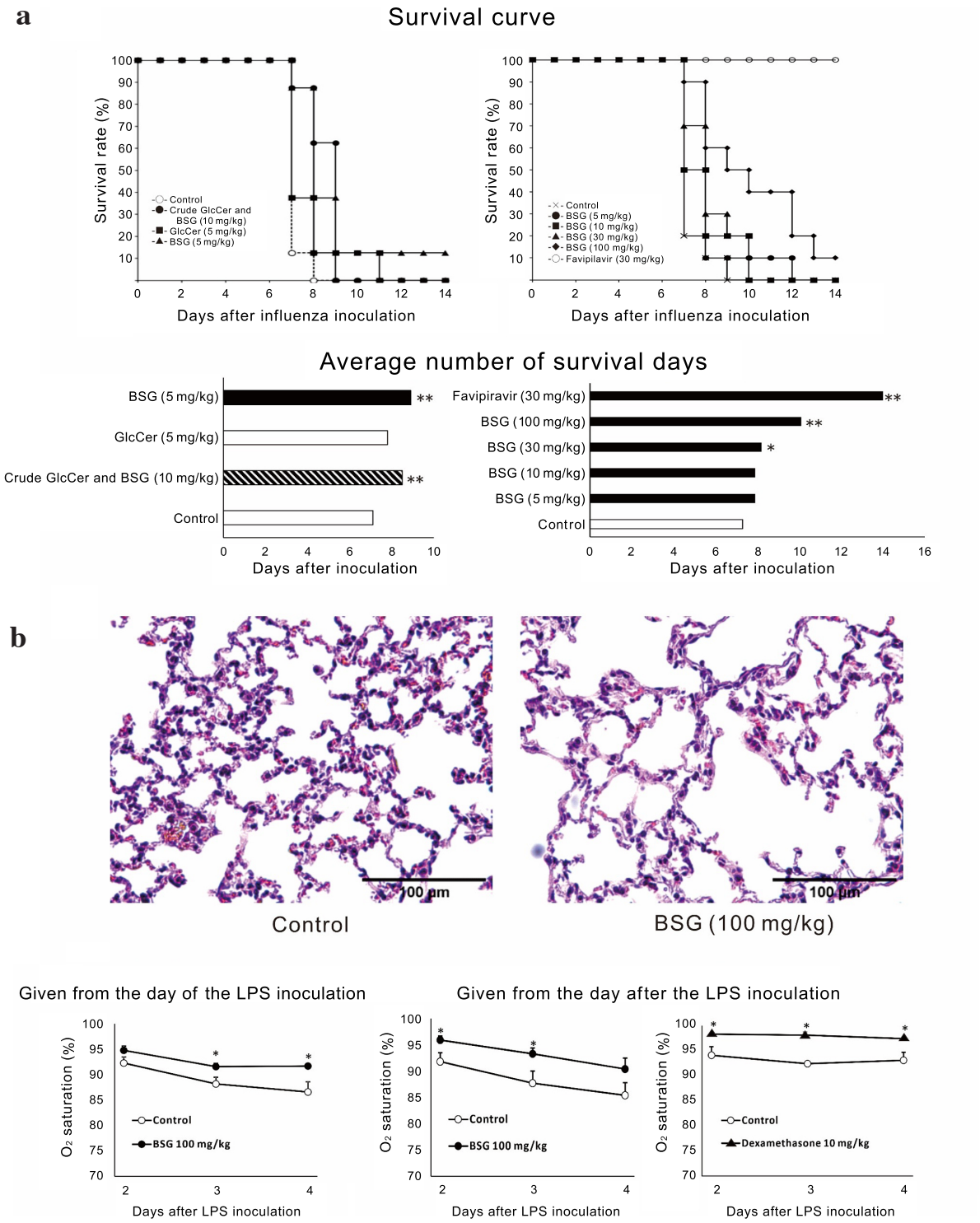

Fig. 9. **Effects of BSG on the survival rate of influenza-infected mice (a), LPS-induced lung neutrophil accumulation (b), and LPS-induced pneumonia (c).**

a) Test samples were orally administered to female BALB/c mice for 7 days and the virus (mutated A/PR/8/34, 7.9×10^6 $TCID_{50}$) was then intranasally inoculated. Test samples were continuously administered once a day and the survival rate was monitored. **b)** BSG was orally administered to male C57BL/6 mice and LPS (1 mg/kg) was intraperitoneally injected. The lungs were removed 24 hr later and specimens were stained by H.E. **c)** BSG or dexamethasone was orally administered to male ICR mice from the day of or the day after the intratracheal administration of LPS (75 μg). Test samples were administered once a day and oxygen saturation was measured for 3 min under anesthesia. Each value represents the mean or mean and SE (n = 5-10). Asterisks denote significant differences from the control at *$p < 0.05$, **$p < 0.01$, respectively. These are unpublished original data. BSG, β-sitosterol glucoside; LPS, lipopolysaccharide; H.E., hematoxylin eosin; SE. standard error.

BSG. A microscopic analysis showed the accumulation of neutrophils. In contrast, BSG (100 mg/kg) suppressed the alveolar accumulation of neutrophils (***Fig. 9-b***). BSG (100 mg/kg) was also orally administered to mice and LPS was intratracheally administered to induce pneumonia. O_2 blood saturation was then measured. BSG prevented reductions in the blood O_2 saturation rate in mice with LPS-induced pneumonia (***Fig.9-c***). These results suggest that BSG non-specifically ameliorated lung inflammation and improved respiratory function.

Conclusion

We herein demonstrated that GlcCer[d18:2(4*E*,8*Z*)] exerted fatty acid length-dependent effects on barrier functions in an epidermis model. The underlying mechanisms appear to involve increasing the density of SC and up-regulating the expression of filaggrin and corneodesmosin. In contrast, Cer[t18:0/24:0] exerted moisturizing effects by promoting the production of SC Cer[NS/NDS] through GCS. Regarding anti-melanogenic effects, GlcCer[d18:2(4*E*,8*Z*)] with C18 or C20 fatty acids and Cer[t18:0/24:0] suppressed melanin production in melanoma cells. Although the inhibitory mechanism of GlcCer remains unclear, the effects of Cer[t18:0/24:0] involved down-regulating the expression of TYRP1 and ATP. Furthermore, BSG not only enhanced skin barrier functions, but also exerted lung protective effects.

Acknowledgments

This work was supported by the New Aichi Creative Research and Development Subsidy (grant numbers: 118-20, 2020) and Oryza Oil & Fat Chemical Co., Ltd.

Conflict of Interest Statement

The authors have indicated no potential conflict of interest.

References

1) Sugawara T, Aida K, Duan J, et al. Analysis of glucosylceramides from various sources by liquid chromatography-ion trap mass spectrometry. *J Oleo Sci*. 2010; 59: 387-394.
2) Tsuji K, Mitsutake S, Ishikawa J, et al. Dietary glucosylceramide improves skin barrier function in hairless mice. *J Dermatol Sci*. 2006; 44: 101-107.
3) Takara T, Yamamoto K, Suzuki N, et al. Oryza ceramide, a rice-derived extract consisting of glucosylceramides and β-sitosterol glucoside, improves facial skin dehydration in Japanese subjects. *Functional Foods Health Disease*. 2021; 11: 385-407.
4) Shimoda H, Terazawa S, Hitoe S, et al. Changes in ceramides and glucosylceramides in mouse skin and human epidermal equivalents by rice-derived glucosylceramide. *J Med Food*. 2012; 15: 1064-1072.
5) Coderch L, López O, de la Maza A, et al. Ceramides and skin function. *Am J Clin Dermatol*. 2003; 4: 107-129.
6) Vávrová K, Henkes D, Strüver K, et al. Filaggrin deficiency leads to impaired lipid profile and altered acidification pathways in a 3D skin construct. *J Invest Dermatol*. 2014; 134: 746-753.
7) Uche LE, Gooris GS, Bouwstra JA, et al. High concentration of the ester-linked ω-hydroxy ceramide increases the permeability in skin lipid model membranes. *Biochim Biophys Acta Biomembr*. 2021; 1863: 183487.
8) Yokose U, Ishikawa J, Morokuma Y, et al. The ceramide [NP]/[NS] ratio in the stratum corneum is a potential marker for skin properties and epidermal differentiation. *BMC Dermatol*. 2020; 20(1): 6.
9) Miyasaka K, Manse Y, Yoneda A, et al. Anti-melanogenic effects of glucosylceramides and elasticamide derived from rice oil by-products in melanoma cells, melanocytes, and human skin. *J Food Biochem*. 2022; 46(10): e14353.
10) Ohta K, Hiraki S, Miyanabe M, et al. Appearance of intact molecules of dietary ceramides prepared from soy sauce lees and rice glucosylceramides in mouse plasma. *J Agric Food Chem*. 2021; 69: 9188-9198.
11) Takeda S, Yoneda A, Miyasaka K, et al. Comparative study on epidermal moisturizing effects and hydration mechanisms of rice-derived glucosylceramides and ceramides. *Int J Mol Sci*. 2022; 24(1): 83.
12) Fernandez ML, Vega-López S. Efficacy and safety of sitosterol in the management of blood cholesterol levels. *Cardiovasc Drug Rev*. 2005; 23: 57-70.
13) Zhou BX, Li J, Liang XL, et al. β-sitosterol ameliorates influenza A virus-induced proinflammatory response and acute lung injury in mice by disrupting the cross-talk between RIG-I and IFN/STAT signaling. *Acta Pharmacol Sin*. 2020; 41: 1178-1196.
14) Takeda S, Terazawa S, Shimoda H, et al. β-Sitosterol 3-*O*-D-glucoside increases ceramide levels in the stratum corneum via the up-regulated expression of ceramide synthase-3 and glucosylceramide synthase in a reconstructed human epidermal keratinization model. *PLoS One*. 2021; 16: e0248150.
15) Fujii M, Shimazaki Y, Muto Y, et al. Dietary deficiencies of unsaturated fatty acids and starch cause atopic dermatitis-like pruritus in hairless mice. *Exp Dermatol*. 2015; 24: 108-113.
16) Rojas M, Woods CR, Mora AL, et al. Endotoxin-induced lung injury in mice: Structural, functional, and biochemical responses. *Am J. Physiol. Lung Cell Mol. Physiol*. 2005; 288: L333-L341.
17) Verhoeven D, Teijaro JR, Farber DL. Pulse-oximetry accurately predicts lung pathology and the immune response during influenza infection. *Virology*. 2009; 390: 151-156.
18) Sybert VP, Dale BA, Holbrook KA. Ichthyosis vulgaris: identification of a defect in synthesis of filaggrin correlated with an absence of keratohyaline granules. *J Invest Dermatol*. 1985; 84: 191-194.
19) Rawlings AV, Harding CR. Moisturization and skin barrier function. *Dermatol Ther*. 2004; 17 (Suppl 1): 43-48.
20) Garrod D, Chidgey M. Desmosome structure, composition and function. *Biochim Biophys Acta*. 2008; 1778: 572-587.
21) Groen D, Gooris GS, Bouwstra JA. Model membranes prepared with ceramide EOS, cholesterol and free fatty acids form a unique lamellar phase. *Langmuir*. 2010; 26: 4168-4175.
22) Fujii M, Shimazaki Y, Nabe T. Diet-induced mouse model of atopic dermatitis. *Methods Mol Biol*. 2021; 2223: 79-86.
23) Hattori F, Ohshima Y, Seki S, et al. Feasibility study of B16 melanoma therapy using oxidized ATP to target purinergic receptor P2X7. *Eur J Pharmacol*. 2012; 695: 20-26.
24) Kim JY, Lee EJ, Seong YJ, et al. AZD-9056, a P2X7 receptor inhibitor, suppresses ATP-induced melanogenesis. *J Dermatol Sci*. 2020; 100: 227-229.